


Digital LIGA: exploitation of droplet-on-demand inkjet printing to fabricate complex mechanical structures by electroforming

Annelies Sels¹ , Remo Blum², Rajasundar Chandran², Enrica Montinaro³, Jan Schildknecht³, Mickael Chabart³ and Vivek Subramanian^{1,4,*}

¹ Institute of Electrical and Micro Engineering, École Polytechnique Fédérale de Lausanne, Lausanne 1015, Switzerland

² iPrint Institute, HEIA-FR, HES-SO University of Applied Sciences and Arts Western Switzerland, Fribourg CH-1700, Switzerland

³ Richemont Manufacture Horlogère ValFleurier, Rue Jaquet-Droz 1, 2000 Neuchâtel, Switzerland

⁴ Department of Electrical Engineering and Computer Sciences, University of California, Berkeley, CA 94720, United States of America

E-mail: Vivek.subramanian@epfl.ch

Received 23 July 2022, revised 8 March 2023

Accepted for publication 10 May 2023

Published 22 May 2023



Abstract

A novel 3D fabrication technique called digital LIGA is proposed, integrating functional digital printing with 3D microfabrication via electrodeposition. This allows for the realization of complex multilevel metallic structures without problems associated with merging growth fronts. To achieve this, we developed a gold nanoparticle ink, compatible with a SU-8 photoresist, for printing the digitally-defined seed layers. Using this ink, selective printing of a conductive seed layer on a multi-level photoresist was used along with subsequent electrodeposition. Defect-free complex multilevel metallic 3D structures were successfully prepared via this method.

Supplementary material for this article is available [online](#)

Keywords: UV-LIGA, gold nanoparticles, inkjet printing, electroforming

(Some figures may appear in colour only in the online journal)

1. Introduction

Electroforming of precision metallic parts is important for a range of industries that depend on micromechanics

or micromotors, including the watch industry and other industries [1–3].

LIGA (German acronym for Lithographie, Galvanoformung, Abformung) is a well-known photolithography-based process, widely used in the industry for such microfabrication [4]. UV-LIGA is a particular variation of LIGA in which a UV illumination source is used in the lithographic process, typically with a thick UV-sensitive photoresist. In UV-LIGA, a deep pattern is made in the photoresist on top of a metallic seed layer. Electroforming is then used to fill the resulting pattern, forming the precision part. The fabrication process produces

* Author to whom any correspondence should be addressed.



Original content from this work may be used under the terms of the [Creative Commons Attribution 4.0 licence](#). Any further distribution of this work must maintain attribution to the author(s) and the title of the work, journal citation and DOI.

metallic structures with thicknesses from a few micrometers to several hundreds of micrometers [5, 6]. A thick photoresist is required to fabricate large-aspect-ratio microstructures with well-defined sidewalls; thick SU-8 is one of the most commonly used photoresists for this application [7].

Currently the LIGA process is limited to fabrication of 2.5D microstructures, producing only single level pieces. However, the demand for more complex, multilevel metallic parts increases for applications like micro gears, miniature medical components or microelectromechanical systems (MEMS) [1, 8–10]. Therefore, there is a need for innovations in the LIGA process to enable multilevel part fabrication.

2. LIGA process overview

Most LIGA processes to date are focused on single level parts, though there have been some demonstrations of multilevel LIGA as well. The comparison between single and multilevel LIGA is shown in figure 1. Traditional UV-LIGA is a result of a series of patterning and deposition steps. Thick SU-8 photoresist is deposited on a conductive layer and patterned using photolithography. A developer is used to dissolve the uncrosslinked photoresist and produce a patterned mold.

Next, the substrate is immersed in an electroplating bath for electroforming in the patterned photoresist to produce the desired metallic pieces. These pieces are released by removal of the photoresist, resulting in single level structures.

Several methods have been studied to develop a LIGA process for more complex multilevel structures; however, significant drawbacks are observed depending on the method chosen.

Multilevel LIGA based on the traditional process has previously been achieved by repeated electrodeposition. Here, the process is repeated using two steps, where the electroformed piece formed during a first step is used as a base substrate for a second electroforming step. This technique however is limited by the overlay accuracy and stress between the metal layers [11]. As such, micrometer-scale precision has been difficult to achieve [12–14].

Non-traditional multilevel LIGA using multi-step resists begins with a very similar procedure to that used in single layer fabrication. Photoresist deposition and lithography result in a patterned photoresist. Next, a second photoresist layer is deposited and patterned, resulting in a two-level photoresist pattern. Electroforming using this template results in two level metallic pieces.

Figure 2(a) depicts the electroformed single (upper) and multi-level (lower) metallic structures after release of the photoresist structure.

To improve the quality and structural integrity of the electroformed pieces in multilevel LIGA, an additional seed layer is required on the multi-level photoresist structure. (figure 2(b)) Physical vapor deposition of seed layers often results in defects, in particular voids or keyholes that reduces the overall mechanical strength of the formed part. (figure 2(c)) Evaporated seed layers coat both horizontal and vertical sides

of the photoresist, resulting in multiple growing fronts. When multiple growing fronts during electrodeposition meet, the final electroformed pieces often include keyholes. This effect can be enhanced due to higher local current density and faster electrodeposition rate at the edges of trenches, better known as the edge effect [16].

These effects limits the complexity of parts currently produced. Although optimization of plating on sputtered seed layers (multi-front) has been studied [15, 17], alternative methods should be considered, since the control of complex 3D growth fronts from a single seed layer is ultimately highly limiting.

Here, a novel 3D fabrication technique called digital LIGA is proposed, integrating functional digital printing with 3D microfabrication that allows for the formation of multilevel structures with independent control of growth fronts during electroforming. The compatibility of inkjet printing and electrodeposition has been evaluated before, and is exploited herein to enable the formation of multilevel parts without the disadvantages of previously proposed multilevel LIGA processes [18, 19].

The concept of digital LIGA is to selectively print a conductive seed layer on a multi-level photoresist, such as SU-8. This eliminates seed layers on the sidewalls of the photoresist and therefore contains only one growing front during electrodeposition. As the growth front progress, it connects to the printed seed layers on upper levels and brings them into the circuit, thus offering the ability to control growth fronts in a highly customized manner based on the needs of the part being electroformed. Electroplating of the first level from the base layer continues to the printed seed layer and a complex two-level structure can be formed. (Figure 2)

Developing this technique requires optimization of several materials and investigation of their compatibility. Here, we report on the overall technology, including materials and printing optimization, process optimization, and on the realization of 3D mechanical parts using digital LIGA-based electroforming.

Digital LIGA depends on the use of a printed seed layer formed by printing ink via inkjet printing in controlled patterns, which in turn are used to direct the growth front. The ink formulation and printing conditions are optimized through choice of solvent and surface modification of the SU8 via oxygen plasma to ensure that the printed ink adequately wets the structures to form continuous layers within the wells of the SU8 pattern. To convert the printed ink into a conductive seed layer, a curing process is required. SU-8 is a well-known negative photoresist which has an onset of thermally induced cross-linking at 150 °C. The hard bake that completes cross-linking of SU-8 is usually executed between 150 °C–250 °C [20]. Hard baking increases the long-term stability and higher chemical resistance of the material, however the cured SU-8 is usually intended for applications where the resist is to be left as part of the final device. In addition, the stress build-up inside the photoresist after curing makes it more likely to peel off from the substrate during electroplating. Therefore, a process using a lower temperature range is needed.

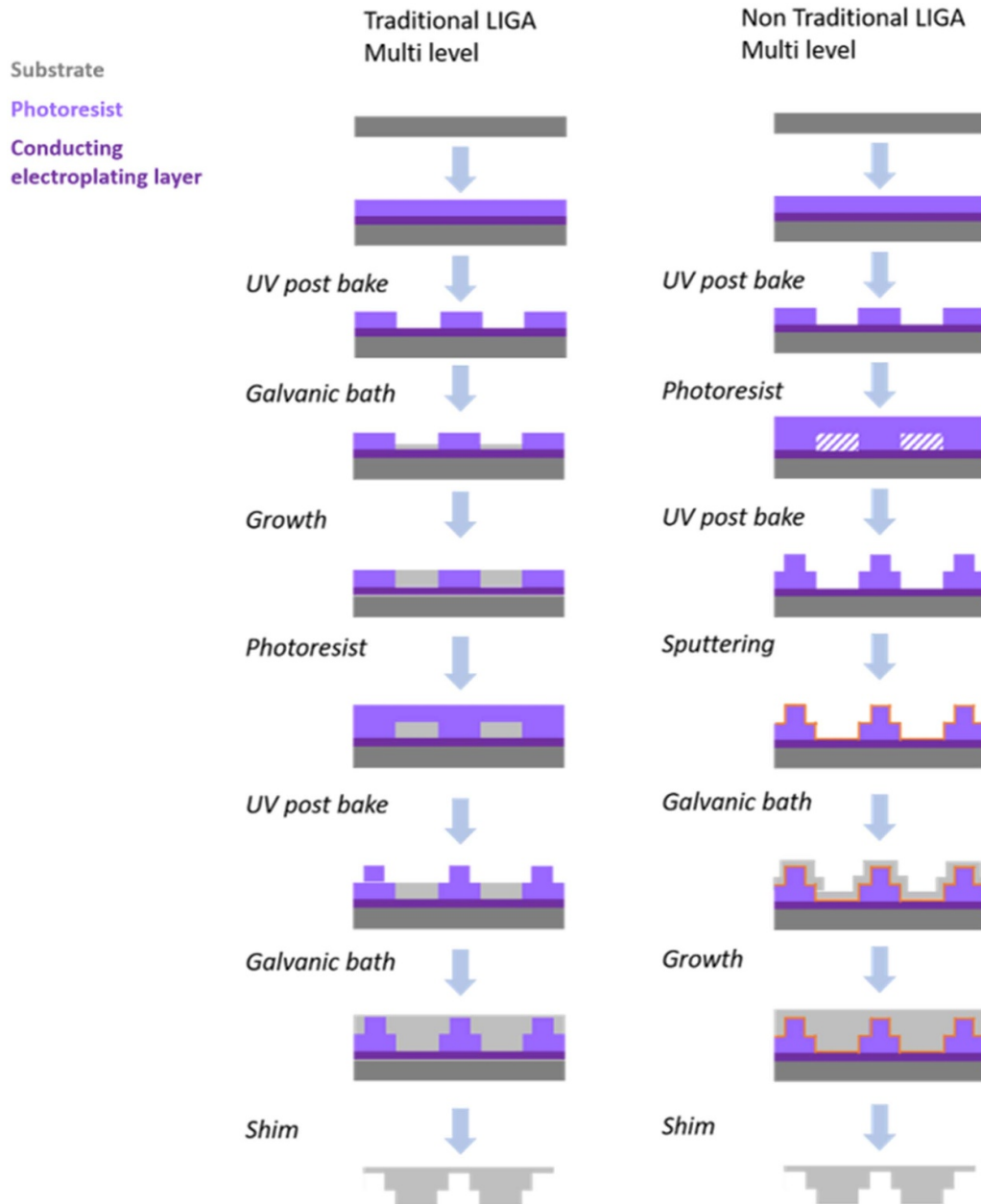


Figure 1. Comparison of single and multi-level LIGA processes.

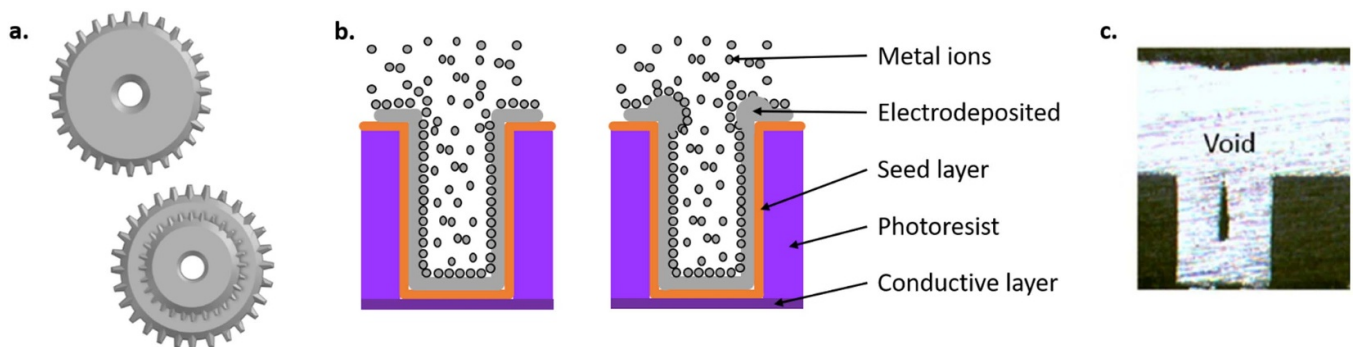


Figure 2. Single and multi-level metallic structures after electroforming (a), seed layer deposition and edge effect (b) and void formation [15] (c). After the void is sealed, growth continues as a unified growth front, deleteriously integrating voids into the released structure. Reproduced from [15]. © The Author(s). Published by IOP Publishing Ltd. CC BY 4.0.

Metal nanoparticles, in comparison to their bulk counterparts, are known to have a significantly lower melting temperature. Several groups have utilized this characteristic to their benefit [21, 22]. We have previously investigated the sintering behavior of silver and gold nanoparticles thoroughly and observed a conversion of the nanoparticles at temperatures as low as 120 °C [23]. The exposure to heat during the conversion process results in out-diffusion of the protecting ligands inside the sintered film, delivering a final film with the requisite conductivity to serve as a seed layer [24].

Integration of these metal nanoparticles in printable inks allows their incorporation in MEMS devices [22, 25–27]. Ligand-protected metal nanoparticles have shown extremely high ink stability. Stability is essential for inkjet printing since unstable and aggregated nanoparticle inks can result in clogged printing nozzles and therefore failure of the printing system. The significant role of the protecting ligands in stability, solubility and curing temperature should be carefully studied and therefore requires optimization in the ink formulation process, as performed herein.

To demonstrate the technique, a seed layer containing gold nanoparticles was printed onto a two level SU-8 structure. The complete structure was sintered and applied in an electrodeposition process. Two level metallic 3D structures were successfully prepared via this method.

3. Experimental details

3.1. Materials

Tetrachloroauric acid trihydrate (Sigma-Aldrich, 99.9%), sodium borohydride (Acros, >98%), Hexanethiol (Sigma-Aldrich, 99%), methanol, dichloromethane and toluene (Fisher scientific, for analysis grade), were used as purchased. Nanopure water (>18 M Ω) was used. All other commercial chemicals were used as received. A copper electroplating bath (H₂SO₄, 10 ± 5 g l⁻¹ and CuSO₄, 15 ± 5 g l⁻¹) was developed. SU-8 3000 (Kayaku Advanced Materials) was used as photoresist.

3.2. Instrumental

TEM analysis was performed on an Osiris Technai (FEI), TGA was performed on a Linseis TGA PT1600; SEM analysis was recorded on a Gemini SEM 450 (Zeiss), confocal imaging and thickness measurements were performed on a 3D-laser microscope VK-X3000 (Keyence).

A Discovery HR-2 rheometer (TA Instruments) was used to determine the viscosity of the inks at 25 °C, varying shear rate between 1–200 l s⁻¹. All pure solvent systems were considered to be Newtonian. Addition of nanoparticles can increase an ink's low shear rate viscosity and lead to non-Newtonian behavior at sufficiently high particle loading (~60%) [28, 29]. However non-Newtonian behavior was not observed during jetting (at shear rates of ~105 l s⁻¹), and thus viscosity values measured at low shear rates were used.

3.3. Mold formation

Two level SU-8 was used to form the mold, similar to processes previously reported. The layer thicknesses of the mold were approximately 200 μ m for each layer, resulting in an overall mold depth of approximately 400 μ m. A 3D profile of an example mold is shown in figure 10(A). Single layer molds were also prepared [30–32].

3.4. Nanoparticle optimization and ink formulation

Thiolate protected gold nanoparticles have a high stability due to the strong gold–sulfur bond and the alkalic chain protecting the particles. There are several types of thiolate ligands with various lengths and bulkiness. Increasing the length of the ligands increases the stability of the particles, however this also increases the quantity of organic material in the ink, resulting in a higher sintering temperature. Hexanethiol (CH₃(CH₂)₅SH) protected gold nanoparticles are ideal candidates that match the temperature requirements for compatible seed layer material.

Therefore, hexanethiol gold nanoparticles (3–5 nm) were synthesized following the Brust method and characterized; see supporting information. Characterization of particle size homogeneity was performed by transmission electron microscope (TEM) (figure 3(a)).

TGA analysis in figure 3(b) monitors the onset temperature at which the organic ligands start to leave the system. This indicates a conversion temperature of the hexanethiol-encapsulated particles of around 150 °C. The maximum allowable temperature is set by the SU-8 cross linking temperature as mentioned before, and therefore these particles are attractive for use in seed layer formation.

Next a suitable ink formulation to incorporate the nanoparticles and be compatible with inkjet printing is required. Therefore, rheometrical studies were performed using combinations of toluene and terpineol with a 15 w% nanoparticle loading. A solvent mixture of 10 w% toluene and 90 w% α -terpineol matched the required viscosity range (15 mPa s) and was able to disperse the nanoparticles well. The ink was also suitable for printing on the SU-8, with adequate wetting to ensure continuous printed patterns.

Printing was performed using a custom-built printer with dimatix DMP piezoelectric inkjet heads. The fly height of the head above the substrate is maintained at approximately 0.5 mm to ensure compatibility with the topography of the substrate. The droplet size on the substrate is found to produce pixels of 20 μ m diameter, which is a sufficient resolution for the parts produced herein. The cone of dispersion of the droplets at this fly height are sufficient to meet pattern accuracy needs herein. We observe that the placement error of individual drops is generally less than 5 μ m, so a printing pattern is selected to ensure an appropriate guard band relative to the mold sidewalls to prevent seed layer encroachment onto the sidewalls. An optical vision system using a digital camera is used to align the inkjet head to the SU-8 pattern.

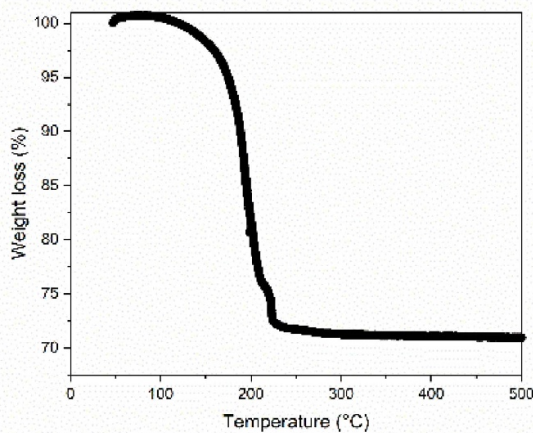
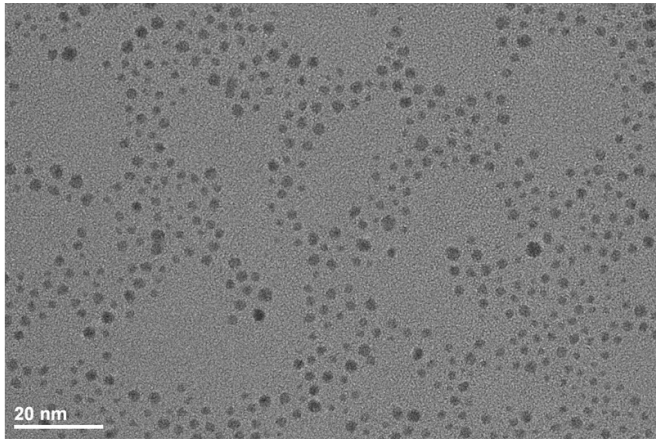


Figure 3. (a) TEM and (b) TGA of hexanethiol protected gold nanoparticles.

3.5. Electroforming

Electrodeposition or electroplating of the optimized printed seed layers was studied using a copper electroplating bath. We note that Nickel and Copper electroplating are both used in such LIGA processes and they can show different growth behaviors depending on the specific bath conditions; here, we focus on production of copper parts. Copper electroplating has been well established and is often used for preliminary electrodeposition studies. Electroplating is a reduction–oxidation (redox) reaction that converts the ions in the plating bath to metal. The reaction is completed by the transfer of electrons from the oxidized to the reduced species. Herein the plating solution consisted of a copper bath (H_2SO_4 , $10 \pm 5 \text{ g l}^{-1}$ and CuSO_4 , $15 \pm 5 \text{ g l}^{-1}$), a copper anode and the printed seed layer functioning as cathode. The reaction was carried out under constant stirring at room temperature.

Electrodeposition was achieved by applying a constant current to the sample immersed in the copper bath. An electroplating rectifier (Galvamat) was used to control the plating current. In order to have the best plating results, well defined

current densities were applied to the samples and increased every 5 min (0.5 A dm^{-2} , 1 A dm^{-2} , 2 A dm^{-2} , 3 A dm^{-2} , 4 A dm^{-2} and 6 A dm^{-2}). In between each increase of current, the sample was removed from the bath, rinsed and deposition was verified.

It was found that all substrates required plasma treatment (3 min, 150 W, O_2 plasma) to remove any remaining encapsulant from the surface and increase surface wettability of the gold seed layer.

The sintered gold layers on partially cured photoresist showed good adhesion to the substrate, even when exposed to the highly acidic copper electroplating bath. A height variation of less than 10% was achieved on the plated squares.

4. Results and discussion

To convert the printed ink into a conductive seed layer, a curing process is required. Thermal exposure of SU-8 results in cross-linking of the photoresist, which can lead to delamination during the LIGA process. Therefore, the compatibility of the photoresist was tested at several thermal cycles.

To confirm the compatibility of the photoresist to these thermal cycles, patterned SU-8 samples were exposed to 175°C for 30 min, analyzed by optical profilometry and electroplated. A 10 nm gold layer was sputtered over the sample to avoid any interference.

Analysis by optical profilometry revealed no real height change (figure 4). In addition, no significant delamination could be observed after electroplating of the samples. It can therefore be concluded that a process temperature below 175°C is imposed for our future sintering studies.

The combination of the SU8 temperature constraints and the sintering requirements of the nanoparticles restricts the temperature range to 150°C – 175°C . To obtain the exact conversion temperatures of hexanethiol gold particles, a systematic study varying both exposure temperature and time was performed.

A gold nanoparticle ink (15 w%, 90–10 α -terpineol-toluene) was inkjet printed on a full SU-8 layer with a film thickness of $0.2 \mu\text{m}$.

The samples were heated at a specific temperature on a hotplate in air, with temperatures varying from 145°C to 165°C with 10 min intervals to measure the resistance by four-point probe measurements (figure 5). The missing points in the graph showed a resistance higher than $50 \Omega/\square$ and were therefore omitted. It can be observed that at 145°C the printed patterns convert into conductive films after approximately 40 min. Since the printed patterns are subsequently used for electroplating, it is desirable to maximize conductivity to reduce non-uniform electroplating due to Ohmic losses in the seed layer.

Increasing the temperature reduces the time needed for conversion; at 165°C the sample is converted after less than 10 min. These values are in the temperature compatibility range of the photoresist.

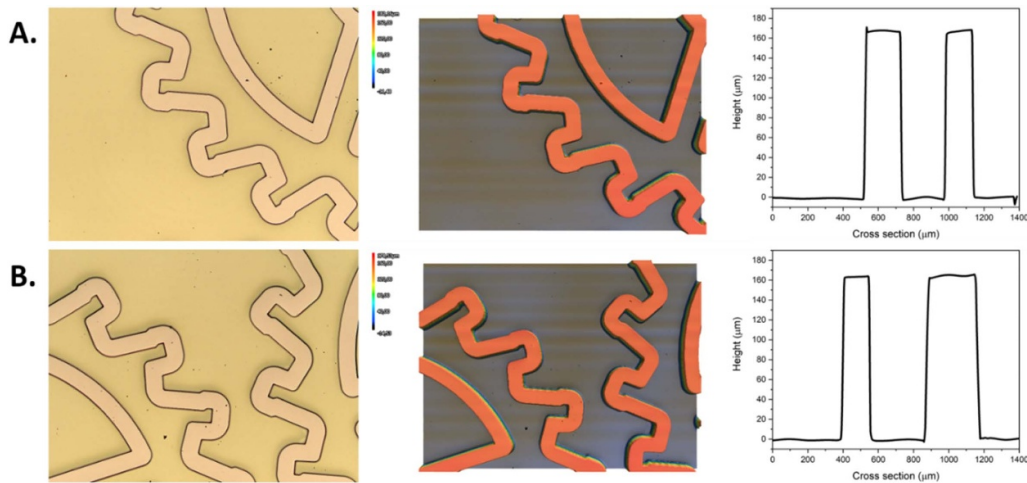


Figure 4. Confocal microscopy images and height profile of the patterned reference sample SU-8 before (A) and after (B) exposure to increased temperatures (175 °C). The samples were sputtered with 10 nm gold to avoid optical interference.

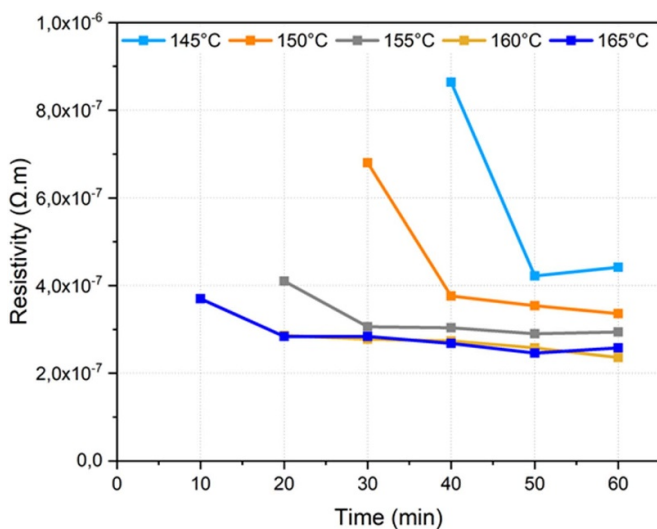


Figure 5. Sintering profile hexanethiol ($n = 6$) gold nanoparticles on SU-8. All samples were sintered on a hotplate in air.

All samples reach around 10% of bulk gold conductivity after full conversion, which is acceptable for electrodeposition and has been found to entirely eliminate Ohmic loss-induced electroplating nonuniformity in the structures fabricated herein.

Once the gold nanoparticles were optimized to be compatible with the photoresist, printing optimization is required to produce good printed seed structures on SU-8. Printing resolution and wetting properties are important to achieve good printing quality inside the SU-8 channels without wetting of the sidewalls. By means of design of experiments (DoE), a systematic study was performed to obtain the ideal printing conditions.

The printing optimization was performed using a Dimatix materials printer (DMP-2800, Dimatix-Fujifilm). The nominal ejection volume of the printhead (DMC-11610, Dimatix-Fujifilm) is 10 pL. The nozzle for ink ejection was

controlled by a bipolar waveform. The nozzle and ink chamber were heated to 40 °C and the printing stage was set at 58 °C.

During this study, the number of layers (2, 3, 4 or 5 printed layers), the drop spacing (15, 20 or 25 μm drop spacing) and the drying methods (every printed layer, every two printed layers or at the end of printing) were varied using a multifactorial DoE. The details of the DOE are included in the supplemental information. After printing and sintering on a hot plate in air, the sample thickness, the sheet resistance and the sintering temperature of the printed film were measured and analyzed. The experimental results were fitted to a second order polynomial using JMP, a commercial DOE tool, and the results were used to select the optimum printing conditions (figure 6). Verification runs were performed at the optimum conditions to validate the predictions; these were then used in the subsequent electroplating work.

No significant influence can be observed by changing the drying method in the printing process. In addition, an increase in the number of printed layers also increases the film thickness while an increasing drop spacing decreases the film thickness, as expected. For these thin films (<1 μm) the film thickness greatly affects the sheet resistance of the printed pattern. Therefore, increased drop spacing increases the sheet resistance of the printed pattern and similarly, an increasing number of layers decreases the sheet resistance slightly. It should be mentioned that the calculated resistivity (Ω m) is very similar for all patterns.

In order to have a sufficiently thick seed layer to meet the conductivity needs of electrodeposition, three printed layers with a drop spacing of 20 μm are selected as parameters for printing these gold nanoparticle inks. These parameters resulted in a continuous layer without defects and sufficient conductance for electrodeposition [33–35].

The edge definition of the printed patterns shows some line edge roughness, but this is not problematic for the LIGA process since the main focus is the wetting of the ink on the surface reaching the edges of the SU-8 sidewalls. Hence the final structure is defined by the SU-8 structure, not the printed

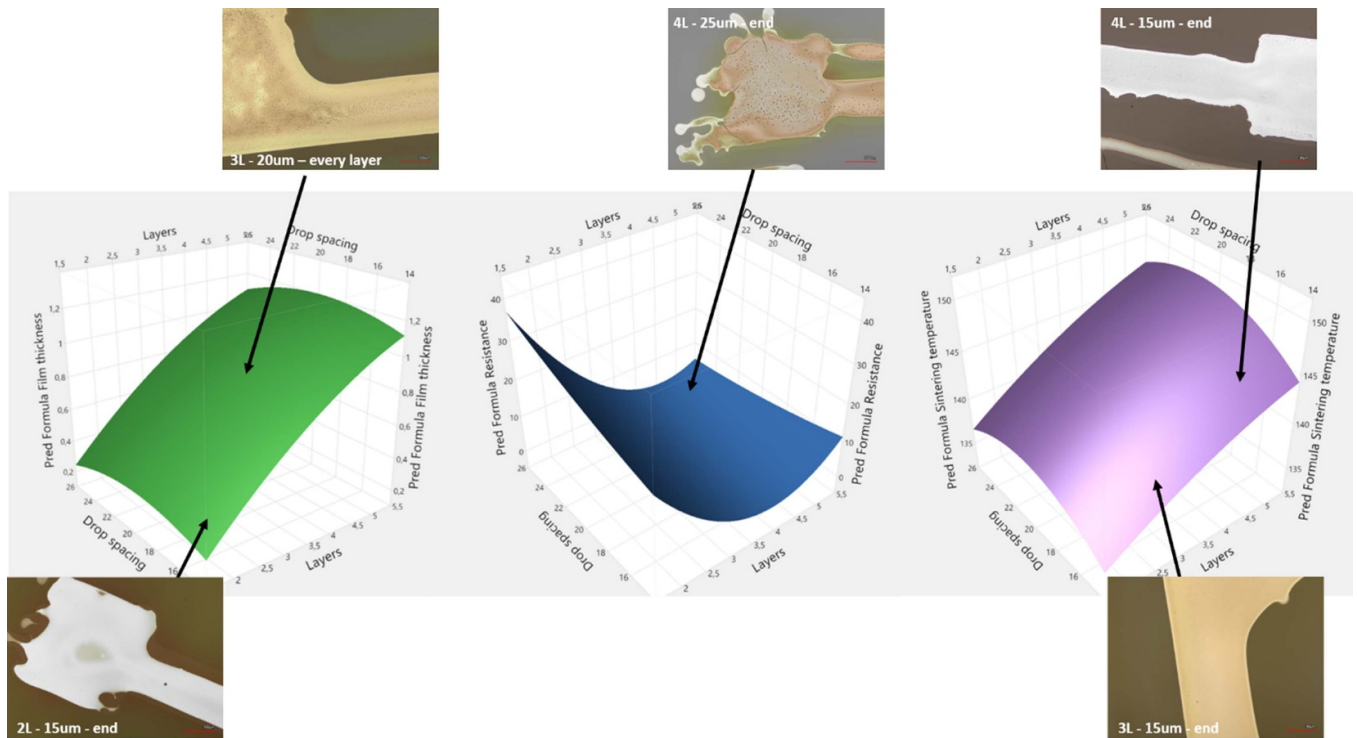


Figure 6. Design of experiments printing conditions overview: the printing optimization varying the number of layers (2, 3, 4 or 5 printed layers), the drop spacing (15, 20 or 25 μm drop spacing) and the drying methods (every printed layer, every two printed layers or at the end of printing). The experimental design is a reduced multifactorial design, and the fitting equation is a second order polynomial. The samples were all dried and sintered on a hotplate in air.

pattern. Note that the minimum feature size of parts produced herein is 200 μm, so the 20 μm inkjet resolution is more than adequate since it is simply necessary to maintain the seed pattern away from the sidewalls to prevent sidewall encroachment of the seed layer. To produce finer features than supported by the 20 μm resolution herein, inkjet heads with higher resolution can be used, along with commensurate alignment accuracy of the printer. As shown in the supporting information, good wetting on the SU-8 can be achieved, resulting in well-defined structures.

4.1. Electroplating of seed layer

Before investigating a multi-level LIGA process, the homogeneity and thickness variation of electrodeposition on the printed seed layers should be studied carefully. Therefore, spiral features of gold seed layers were printed onto full layers (partially cured) SU-8, followed by sintering, plating and evaluation.

The printed spiral samples were exposed to different temperatures (145 °C–175 °C) for 10 and 30 min and electroplated using similar conditions as before. In general, a sheet resistance below 50 Ω/□ is needed for successful plating.

Analysis of the thickness variation on the successfully plated samples was performed via optical profilometry.

Figure 7 shows a homogeneous sintered seed layer with a thickness of 0.35 μm on a full layer of SU-8. The spirals were electroplated 6 times for 5 min, gradually increasing

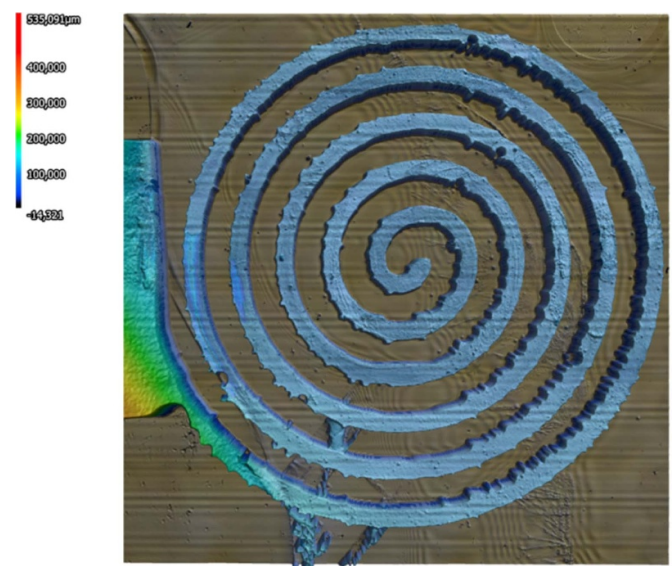


Figure 7. Thickness variation over electroplated spiral.

the current density from 0.5 A dm⁻² to 6 A dm⁻² resulting in an average deposition of 26 μm. Figure 8 indicates the thickness variation between the outer part of the spiral, middle and inner part. A height variation of less than 10% was achieved. It can thus be concluded that a printed gold layer on SU-8 is able to act as a seed layer for electroplating without

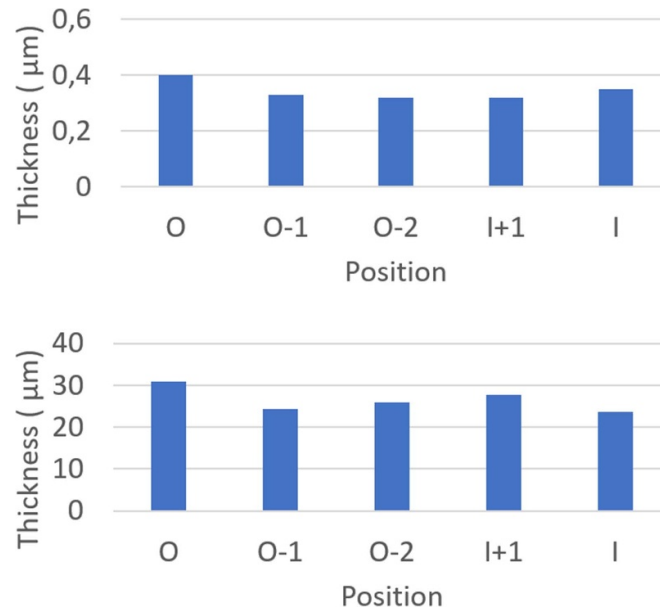


Figure 8. Thickness variation over electroplated spiral on the outer ring (*O*) to the inner ring (*I*) of the sintered (upper) and plated (lower) spirals.

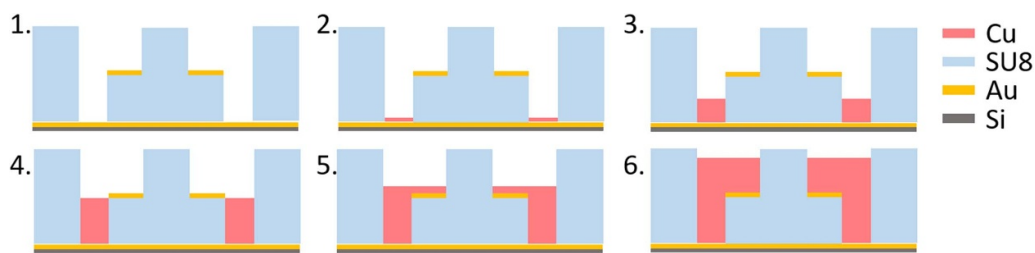


Figure 9. Schematic representation of the two-level structure formation as a series of images representing the progression with time. Step 1 shows the initial mold and seed structure and the subsequent steps show the progress with electrodeposition. The seed layer is only printed on top of the first SU8 level (Step 1). As the electrodeposition progresses (Steps 2–3), the seed layer stays electrically disconnected until the growth front touches it (Step 4). At that point, the seed layer is connected into the circuit and growth proceeds over the entire structure (Step 5) to fill the mold (step 6).

significant Ohmic losses, and can thus deliver good seeding uniformity.

4.2. Two-level structure formation

A demonstrator for the Digital LIGA process is achieved by integrating the optimized printing process into a multilevel photoresist pattern. Figure 9 shows a schematic representation of the two-level structure formation.

A two-level photoresist pattern, with each level approximately 200 µm in height, was sequentially deposited via lithography onto a gold coated silica wafer. The gold coating serves as an initial seed layer in the electrodeposition process. The optimized gold nanoparticle ink was printed as a second seed layer onto a finalized two-level structure photoresist, more specifically on the surface of the first layer of SU-8 (figure 9).

Deposition of the printed seed layer is optimized to prevent sidewall encroachment of the printed pattern since overflow of ink onto the sidewalls of SU-8 will result in formation of multiple growing fronts. By reducing the printed pattern,

calculating for a drop size of 20 µm and a droplet placement precision of 5 µm, successful printing of gold nanoparticles on the SU-8 is observed. Specifically, the patterns are pulled back from the mold edges by one pixel width to ensure no sidewall encroachment. These samples were sintered to convert the gold ink into a seed layer.

The sintered samples were immersed inside a copper electrodeposition bath and connected to the set-up. Once a current is applied, copper is deposited onto the base gold layer. The deposited copper ideally grows inside the SU-8 channel until it reaches the printed gold layer at the second level. If no ink is spilled on the sidewall during printing, homogeneous growth of copper can be achieved.

Figure 10 shows the height profile during this deposition process. It should be noted that the step height of every layer is approximately 200 µm, however due to the interaction of the optical profilometer with transparent SU-8 this height can vary slightly. After 25 min immersion in the copper bath, deposition of a few micrometers is observed only on the gold base layer. Increasing deposition time, continued gradual deposition on

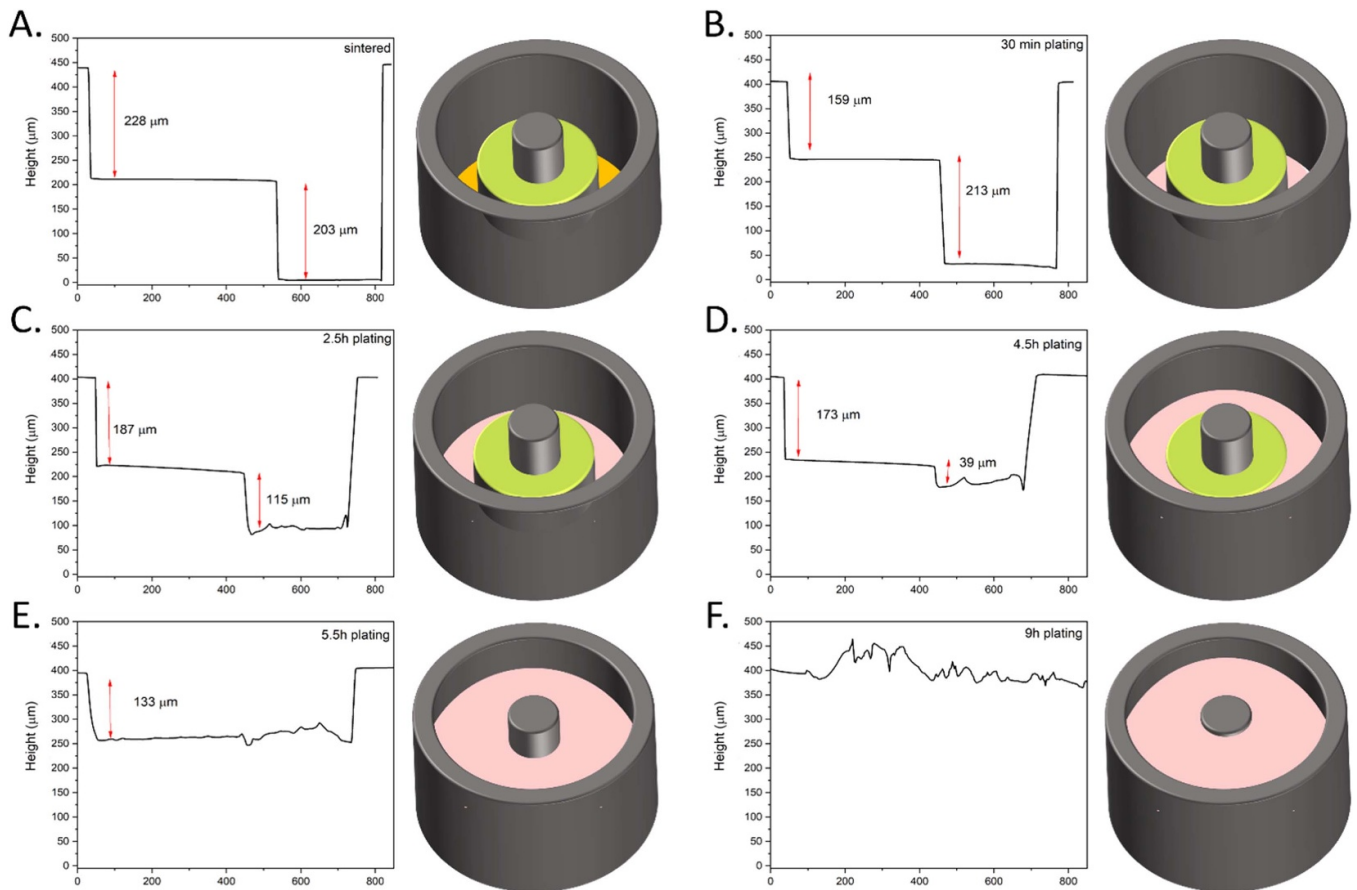


Figure 10. Cross sections during electroplating.

the gold base layer proceeds, which translates into a decrease in the observed step height. After 4.5 h of deposition, copper reaches the printed seed layer. Copper deposition on the seed layer only commences when copper of the gold base layer reached the same level and establishes an electrical connection.

Further deposition for 9 h results in a plated structure of 400 μm , filling the complete multi-level photoresist structure. We note that there is still some non-uniformity of the final piece due to incomplete optimization of the electrodeposition conditions; it is known that uniformity and growth quality is influenced by the electrodeposition conditions such a voltage and stirring speed [16]. Note the complete absence of problems with merging growth fronts, etc, attesting to the benefits of designed seed layers delivered by the digital LIGA process herein. Specifically, since the LIGA process here eliminates sidewall seed layers, we do not see any problems with merging due to sidewall growth fronts; specifically, SEM analysis in figure 11 does not show keyholes. We note that this structure, with a base width of 200 μm and a height of 200 μm in the lower level would be expected to show a keyhole due to any potential merging of sidewall fronts beginning at approximately 50% of the way through the growth. This is not observed herein, attesting to the presence of single growth front, as further evidenced by the time sequence of the cross-sections in figure 10.

4.3. Release of structure

Once the electroforming process is completed and the pieces are plated completely up to the top of the structure, the electrodeposition is stopped and the structures are released.

The release of the structures is achieved by dissolution of the Si substrate in a KOH bath. The SU-8 mold was then mechanically separated from the metal microstructures.

To inspect the quality of the plated structure and the interface of the gold seed layer, the structures were mechanically polished and SEM analysis was performed (figure 11).

Cross-sectional images of the electrodeposited structures indicate that copper electrodeposition was successful and no voids or seams are observed. The interface where the first electroplating front reaches the printed layer on the SU-8 layer, does not show any defects in the structure.

The quality of the copper formed on the printed seed layer is comparable to that formed on the sputtered seed layer. In addition, the edges of the electroplated piece follow exactly the pattern of the SU-8; no defects are observed. Therefore, the final electroplated structure matches the expected structure as depicted in figure 11.

It can therefore be concluded that the digital LIGA process was successful, resulting in a high quality electroplated structure.

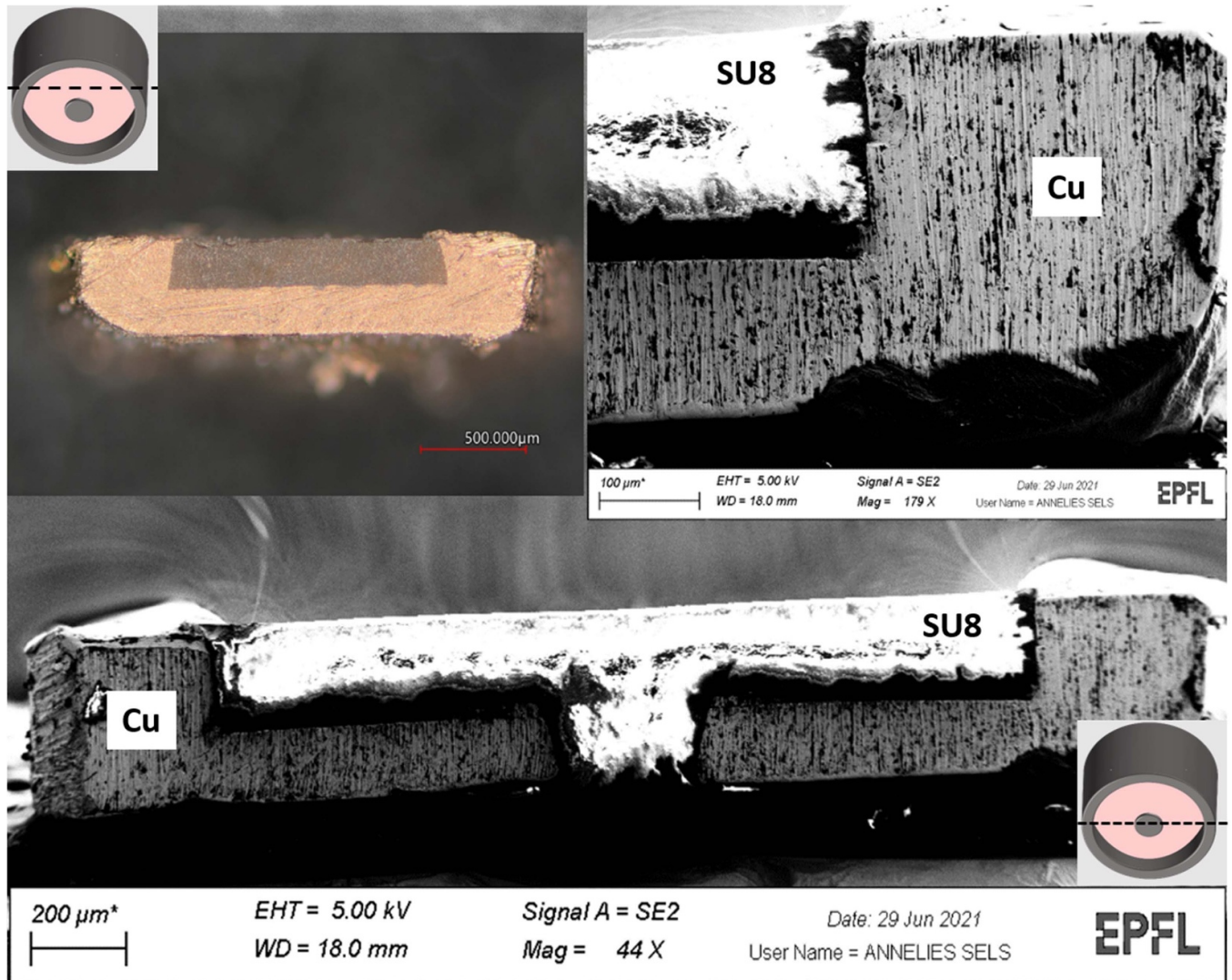


Figure 11. Optical microscope (upper, left) and SEM images of cross-section of the features electrodeposited. Note that all the images are inverted relative to the donut schematic of figures 9 and 10. The optical micrograph shows a cross-section out of plane of the central post as indicated in the inset, and show the formation of continuous copper on the second level of the pattern. The SEM micrographs show a cross-section including the central post. A detailed (zoomed) image of the final piece (upper, right) confirms the absence of voids or seams.

5. Conclusion

By combining UV-LIGA and inkjet printing of a digitally-defined seed layer formed from printed gold nanoparticles, we have demonstrated a straightforward microfabrication method resulting in high-quality complex multilevel metallic parts.

A low temperature sintering gold nanoparticle ink, compatible with the curing of a photoresist, was developed. Printing optimization of this ink onto SU-8 was achieved. Inkjet printing of the seed layer allows control of the growth fronts during electroplating by connecting portions of the seed layer into the electrodeposition circuit mid-growth to prevent the merging of competing growth fronts, which are the cause of common defects during electroplating such as the keyhole problem. This process has thus allowed for realization of two-level metallic structures.

This technique is thus a good candidate for production of complex multi-level metallic parts, especially for microfabrication of precision mechanical components.

Data availability statement

The data that support the findings of this study are openly available at the following URL/DOI: [10.5281/zenodo.7893304](https://doi.org/10.5281/zenodo.7893304).

Acknowledgments

This project was partially funded through the Innosuisse IMPULSE Project 35702.1 IP-ENG.

ORCID iD

Annelies Sels  <https://orcid.org/0000-0002-7032-3978>

References

- [1] Piottter V, Klein A, Plewa K, Guttmann M and Winkler F 2020 Development of stacked conductive templates for electroforming of multi-level metallic micro components *Microsyst. Technol.* **26** 1585–90
- [2] Saile V, Wallrabe U, Tabata O and Korvink J G 2009 *LIGA and its applications* vol (Advanced Micro and Nanosystems vol 7) ed S Volker, W Ulrike, T Osamu and K Jan G (Hoboken, NJ: Wiley) (<https://doi.org/10.1002/9783527622573>)
- [3] Lutttge R 2016 *Advanced Microfabrication Methods, in Nano- and Microfabrication for Industrial and Biomedical Applications* 2nd edn, ed R Lutttge Micro and Nano Technologies (Norwich, NY: William Andrew Publishing) ch 3, pp 55–86
- [4] Malek C K and Saile V 2004 Applications of LIGA technology to precision manufacturing of high-aspect-ratio micro-components and -systems: a review *Microelectron. J.* **35** 131–43
- [5] Williams J D and Wang W 2004 Study on the postbaking process and the effects on UV lithography of high aspect ratio SU-8 microstructures *Proc. SPIE* **3** 563
- [6] Lorenz H, Despont M, Vettiger P and Renaud P 1998 Fabrication of photoplastic high-aspect ratio microparts and micromolds using SU-8 UV resist *Microsyst. Technol.* **4** 143–6
- [7] Zhang H, Zhang N, Gilchrist M and Fang F 2020 Advances in precision micro/nano-electroforming: a state-of-the-art review *J. Micromech. Microeng.* **30** 103002
- [8] Vidyaa V, Kanthababu M, Thilagar S H and Balasubramanian R 2018 Evaluation of macro sized metal based microgrippers for handling microcomponents *Precis. Eng.* **54** 403–11
- [9] Li H 2016 Microfabrication techniques for producing freestanding multi-dimensional microstructures *Microsyst. Technol.* **22** 223–37
- [10] Li X, Ming P, Ao S and Wang W 2022 Review of additive electrochemical micro-manufacturing technology *Int. J. Mach. Tools Manuf.* **173** 103848
- [11] Ma Y, Liu W and Liu C 2019 Research on the process of fabricating a multi-layer metal micro-structure based on UV-LIGA overlay technology *Nanotechnol. Precis. Eng.* **2** 83–88
- [12] Morales A M and Domeier L A 2002 Cantilevered multilevel LIGA devices and methods *U.S. Patent* 6,458,263
- [13] Wang Q, Duan Y, Ding Y, Lu B, Xiang J and Yang L 2009 Investigation on LIGA-like process based on multilevel imprint lithography *Microelectron. J.* **40** 149–55
- [14] Han D, Yamada Y, Yokota S and Kim J-W 2020 Multilayer fabrication of micromolding and electroforming with the planarization of grinding for high-aspect-ratio microelectrodes in electro-conjugate fluid (ECF) micropumps *Int. J. Precis. Eng. Manuf.* **21** 927–36
- [15] Lim C S, Niwa T, Watanabe S, Zhang C, Guan A, Mitsuoka Y and Sato H 2021 Fabrication of void-free submillimeter-scale nickel component by bottom-up electrodeposition *J. Phys. Commun.* **5** 025001
- [16] Ahn J, Hong S, Shim Y-S and Park J 2020 Electroplated functional materials with 3D nanostructures defined by advanced optical lithography and their emerging applications *Appl. Sci.* **10** 8780
- [17] Noda D and Hattori T 2010 Fabrication of microcoils with narrow and high aspect ratio coil line *Adv. Robot.* **24** 1461–70
- [18] Zhou B, Su B, Li M and Meng J 2020 Microelectroforming of freestanding metallic microcomponents using silver-coated poly(dimethylsiloxane) molds *J. Micromech. Microeng.* **30** 045013
- [19] Meissner M V, Spengler N, Mager D, Wang N, Kiss S Z, Höfflin J, While P T and Korvink J G 2015 Ink-jet printing technology enables self-aligned mould patterning for electroplating in a single step *J. Micromech. Microeng.* **25** 065015
- [20] Ceyssens F and Puers R 2012 SU-8 photoresist *Encyclopedia of Nanotechnology* ed B Bhushan (Dordrecht: Springer) pp 2530–43
- [21] Naghdi S, Rhee K, Hui D and Park S 2018 A review of conductive metal nanomaterials as conductive, transparent, and flexible coatings, thin films, and conductive fillers: different deposition methods and applications *Coatings* **8** 278
- [22] Nayak L, Mohanty S, Nayak S K and Ramadoss A 2019 A review on inkjet printing of nanoparticle inks for flexible electronics *J. Mater. Chem. C* **7** 8771–95
- [23] Huang D, Liao F, Molesa S, Redinger D and Subramanian V 2003 Plastic-compatible low resistance printable gold nanoparticle conductors for flexible electronics *J. Electrochem. Soc.* **150** G412
- [24] Volkman S K, Yin S, Bakhishev T, Puntambekar K, Subramanian V and Toney M F 2011 Mechanistic studies on sintering of silver nanoparticles *Chem. Mater.* **23** 4634–40
- [25] Magdassi S 2009 *The Chemistry of Inkjet Inks* ed M Shlomo (Singapore: World Scientific) (<https://doi.org/10.1142/6869>)
- [26] Richter M, Beckenbach T, Daerr H, Prevrhal S, Börner M, Gutekunst J, Zangi P, Last A, Korvink J G and Meyer P 2022 Investigation on the mechanical interface stability of curved high aspect ratio x-ray gratings made by deep x-ray lithography *J. Micro/Nanopatterning Mater. Metrol.* **21** 024901
- [27] Dutta S and Pandey A 2021 Overview of residual stress in MEMS structures: its origin, measurement, and control *J. Mater. Sci.* **32** 6705–41
- [28] Nallan H C et al 2014 Systematic design of jettable nanoparticle-based inkjet inks: rheology, acoustics, and jettability *Langmuir* **30** 13470–7
- [29] Wagner N J and Brady J F 2009 Shear thickening in colloidal dispersions *Phys. Today* **62** 27–32
- [30] Lee J A, Lee S W, Lee K-C, Park S I and Lee S S 2008 Fabrication and characterization of freestanding 3D carbon microstructures using multi-exposures and resist pyrolysis *J. Micromech. Microeng.* **18** 035012
- [31] Mata A, Fleischman A J and Roy S 2006 Fabrication of multi-layer SU-8 microstructures *J. Micromech. Microeng.* **16** 276
- [32] Francisco P et al 2011 Microsystem technologies for biomedical applications *Biomedical Engineering, Trends in Electronics* ed N L Anthony (Rijeka: IntechOpen) ch 3
- [33] Woo T-G, Park I-S and Seol K-W 2009 Effects of various metal seed layers on the surface morphology and structural composition of the electroplated copper layer *Met. Mater. Int.* **15** 293–7
- [34] Frost G and Ladani L 2020 Development of high-temperature-resistant seed layer for electrodeposition of copper for microelectronic applications *J. Electron. Mater.* **49** 1387–95
- [35] Reyes Tolosa M D, Alajami M, Montero Reguera A E, Damonte L C and Hernández-Fenollosa M A 2019 Influence of seed layer thickness on properties of electrodeposited ZnO nanostructured films *SN Appl. Sci.* **1** 1245